NRC Publications Archive
Archives des publications du CNRC

Deformable and durable phantoms with controlled density of scatterers
Bisaillon, Charles-Étienne; Lamouche, Guy; Maciejko, Romain; Dufour, Marc; Monchalin, Jean-Pierre

NRC Publications Record / Notice d'Archives des publications de CNRC:
https://nrc-publications.canada.ca/eng/view/object/?id=e15eb250-2767-4d4f-b301-51545cf85556
https://publications-cnrc.canada.ca/fra/voir/objet/?id=e15eb250-2767-4d4f-b301-51545cf85556

Questions? Contact the NRC Publications Archive team at
PublicationsArchive-ArchivesPublications@nrc-cnrc.gc.ca. If you wish to email the authors directly, please see the first page of the publication for their contact information.

Vous avez des questions? Nous pouvons vous aider. Pour communiquer directement avec un auteur, consultez la première page de la revue dans laquelle son article a été publié afin de trouver ses coordonnées. Si vous n'arrivez pas à les repérer, communiquez avec nous à PublicationsArchive-ArchivesPublications@nrc-cnrc.gc.ca.

National Research Council Canada   Conseil national de recherches Canada

Canada

NOTE

Deformable and durable phantoms with controlled density of scatterers

Charles-Etienne Bisaillon[1,2]**, Guy Lamouche**[1,2]**, Romain Maciejko**[2]**, Marc Dufour**[1] **and Jean-Pierre Monchalin**[1]

[1] Industrial Materials Institute, National Research Council Canada, 75 de Mortagne, Boucherville, Québec J4B 6Y4, Canada
[2] Optoelectronics Laboratory, Engineering Physics, Ecole Polytechnique de Montréal, PO Box 6079, Station 'Centre-ville' Montréal, Québec H3C 3A7, Canada

E-mail: charles-etienne.bisaillon@cnrc-nrc.gc.ca, guy.lamouche@cnrc-nrc.gc.ca, marc.dufour@cnrc-nrc.gc.ca, jean-pierre.monchalin@cnrc-nrc.gc.ca and romain.maciejko@polytml.ca

Abstract

We have developed deformable and durable optical tissue phantoms with a simple and well-defined microstructure including a novel combination of scatterers and a matrix material. These were developed for speckle and elastography investigations in optical coherence tomography, but should prove useful in many other fields. We present in detail the fabrication process which involves embedding silica microspheres in a silicone matrix. We also characterize the resulting phantoms with scanning electron microscopy and optical measurements. To our knowledge, no such phantoms were proposed in the literature before. Our technique has a wide range of applicability and could also be adapted to fabricate phantoms with various optical and mechanical properties.

1. Introduction

The tissue properties that a phantom should simulate depend on the measurement system and specific objectives of an experimental protocol. Our main interest lies in the study of speckle statistics in optical coherence tomography (OCT). OCT is an optical interferometric imaging technique that relies on the coherence of light to trace the scattering profile of a biological tissue. The technique has many applications in the biomedical domain (Bouma and Tearney 2002), and to a lesser extent in the industrial domain (Dufour *et al* 2005). Speckle is an interferometric phenomenon that occurs whenever light waves travel different optical path lengths with a difference smaller than the coherence length of the source. It is very frequent to

observe speckle in OCT images, especially when imaging scattering media such as biological tissues.

Recent studies on speckle in OCT revealed the possibility of identifying tissue properties using texture analysis or speckle statistics from OCT images. First, Gossage *et al* used a set of second-order statistics to produce a tissue classification algorithm. They obtained some success in differentiating various tissues and tissue phantoms, but the study was not directly related to an OCT model of image formation (Gossage *et al* 2003, 2006). More recently, Hillman *et al* have shown a variation of the contrast ratio with the effective number of scatterers (ENS), which is an index representing the average number of discrete scatterers contained within the OCT probed volume (Hillman *et al* 2006). Our goal was to investigate if further information could be obtained from the speckle size. The speckle size is a second-order statistical parameter whose variation can easily be understood. We were thus looking for phantoms that were solid and durable, and that contained a controlled density of scatterers. The durability is a challenging request that allows experiments to be repeated at will. Additionally, by requiring phantoms to be deformable, they can also be used for work on elastography. Elastography measurements in OCT usually rely on speckle tracking and are best done with phantoms that provide a well-defined speckle field. To our knowledge, no fabrication technique proposed in the literature can provide phantoms combining all of these properties. We therefore developed our own procedure using a mixture of silica microspheres in a curing silicone matrix.

In section 2, we review some previous approaches for tissue phantom fabrication that have their own merits but do not satisfy all of our needs. In section 3, we describe our method for mixing silica microspheres in silicone. In section 4, we present characterization experiments that were carried out to assess the quality of our phantoms. In section 5, we discuss the advantages and disadvantages of our innovative technique and provide some suggestions for its adaptation to satisfy the needs of other experiments.

2. Background

A number of combinations of matrices and scattering materials previously reported in the literature were of interest for our type of work. They can be divided into two classes: inorganic powders in silicone and microspheres in water, gelatin or other matrices.

2.1. Inorganic powders in silicone

Room temperature vulcanizing (RTV) silicones are materials often used to simulate the elastic properties of some biological tissues (Jiang *et al* 2003). They are viscous liquids made of polyorganosiloxanes that crosslink when a catalyst is added. Non-organic absorbents and scatterers, like alumina (Al_2O_3) and titanium dioxide (TiO_2) powders, can be added to reproduce the optical properties of various tissues. The values of the absorption coefficient (μ_a), the scattering coefficient (μ_s) and the anisotropy factor (g) of the phantoms can even be predicted with some success using an extension of the Mie scattering theory (Beck *et al* 1998, Lualdi *et al* 2001).

The interesting characteristics of this type of phantom are deformability, solidity, durability and the possibility of reproducing specific tissue properties and shapes. However, even with very high quality samples, inorganic powders always cover a wide range of particle sizes and shapes. This is illustrated in the scanning electron microscope (SEM) image of an alumina powder presented in figure 1. With such a distribution of scatterer sizes, it is almost impossible to obtain a precise evaluation of the density of scatterers. Furthermore, the signal scattered by the particles depends on their size and shape. Therefore, the scattering signal
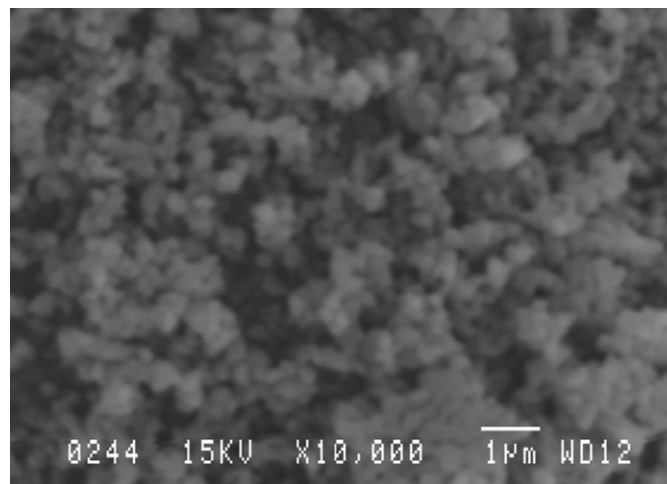
Figure 1. SEM image of an alumina powder. The nominal diameter is 1 μm.

cannot be obtained with a simplified model considering the range of sizes and shapes of the particles found in a powder. A better knowledge of the properties of the scatterers can be gained by using microspheres.

2.2. Microspheres in various matrices

In order to allow a variation in the number of scatterers contained within the probed volume of OCT measurements, the microspheres must have a diameter smaller than the OCT resolution length. Since this length is typically of 10–15 μm, microspheres smaller than 3 μm are required. The use of microspheres this small in size allows for the shape, size and density of all scatterers to be controlled. This leads to phantoms that are easier to model. This is very useful for exploratory work like the study of speckle in OCT. This was the choice made by Hillman *et al* in their work on contrast in OCT using phantoms made of polystyrene microspheres in water (Hillman *et al* 2006). In water, the microspheres move constantly due to the Brownian motion. This changes the microstructure between every A-scan (in depth). These changes do not affect first-order statistical parameters, but they must be avoided for the study of the speckle size, which is a second-order statistical parameter that requires the combined information from adjacent depth scans. It is therefore imperative to use a solid phantom for the study of the speckle size.

In their work on tissue differentiation with texture analysis in OCT, Gossage *et al* solved this issue by using gelatin to solidify water suspensions of silica microspheres (Gossage *et al* 2006). However, the group reported some scattering signal from the gelatin itself which does not give a clear understanding of the nature and exact density of scatterers. As such, a transparent matrix for our phantoms was required. Another disadvantage of the microsphere–gelatin phantoms is their short period of conservation. The two same problems arise in the use of an agar–agar gel to solidify microspheres suspensions, another previously proposed solution (Pogue and Patterson 2006).

Microspheres were also mixed in matrices of polyester (Firbank and Delpy 1993) and epoxy resin (Firbank *et al* 1995). Although these solutions produce durable and solid phantoms with a good control over the density of scatterers, the hardness of the matrices is not suitable to simulate the mechanical behavior required in elastography studies. To our knowledge,
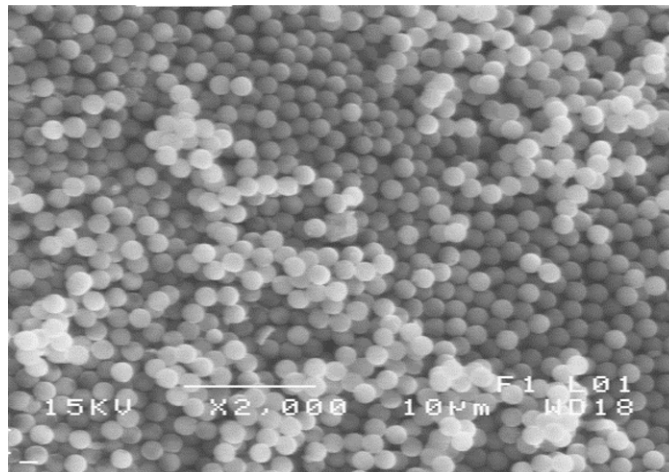
Figure 2. SEM image of dried silica microspheres. The average diameter is 1.86 μm.

phantoms with discrete scatterers as simple as microspheres in a solid, durable and deformable matrix have never been reported before.

3. Methodology

In order to obtain this useful combination of properties, we mixed microspheres in a RTV silicone. This mixing proved to be quite challenging. Microspheres are normally sold in aqueous suspensions. The most common microspheres of sufficiently small dimensions are made of polystyrene, and so, water is effective in preventing aggregation since it creates an electrostatic equilibrium. However, silicone is highly hydrophobic. Our approach is to use silica microspheres in dry form and re-suspend them, while avoiding the use of water. The refractive index of the microspheres is about 1.43–1.45 (according to Bangs Laboratories), which is in the range of indices reported for biological tissues (Tuchin 2000) and their specific gravity is $\rho = 1.96$ g ml^{-1}. Figure 2 shows an SEM image of silica microspheres with an average diameter of 1.86 μm and approximate deviation of 10%. The regularity in size and shape is quite good and thus the microspheres can be considered as discrete spherical scatterers.

The silicone used is Sylgard 184 sold as a resin–catalyst kit mixed in a 10:1 ratio. The product cures in 48 h at room temperature and the reaction can be dramatically accelerated when heated. At the 1.3 μm wavelength used in our OCT system, the silicone is transparent and we measured its group refractive index from OCT images. The ratio of the optical to the geometrical paths yields a group refractive index of $n_s = 1.41$.

The fabrication process begins by weighing the microspheres and by adding the needed volume of the resin. To ensure complete incorporation of the microspheres, the same volume of hexane is added. Hexane is a very good solvent for poly(dimethyl siloxane) (PDMS) and greatly decreases the mixture viscosity (Yang *et al* 2000). This mixture is then placed in an ultrasonic bath for about 2 h, breaking most aggregates, and efficiently and uniformly dispersing the microspheres in the silicone matrix. Afterward, the hexane is evaporated under vacuum for a few hours, leaving the silicone still capable of polymerization. Transparency and group refractive index measurements carried out on blank silicone samples produced with
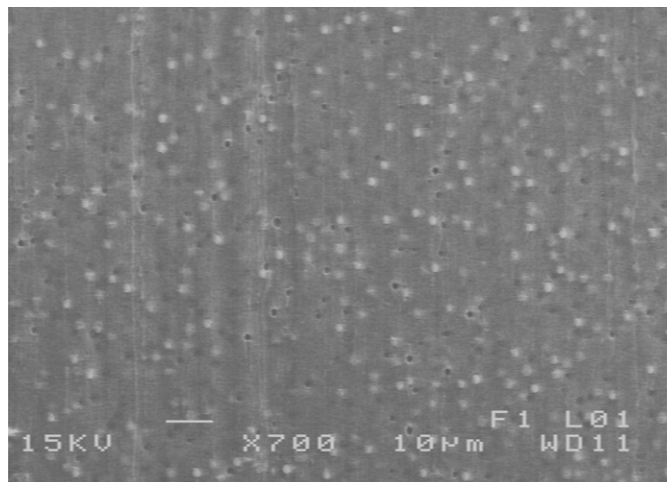
Figure 3. SEM image of a phantom containing 7×10^9 part ml^{-1} of 2.34 μm silica microspheres.

hexane dissolving and ultrasonic bathing showed no significant influence of the process on these optical properties of the matrix. At this point, the proper proportion of reactive is added to the batch and mixed manually. This mixture can be cast in molds of any shape and left aside for polymerization. We typically produced phantoms using 3 ml of silicone resin, 0.3 ml of reactive and from 25 to 300 mg of microspheres. The mixture was cast in cylindrical molds with a diameter of 3.2 cm and removable bottoms. Considering that a certain volume is lost during casting, the phantoms are usually about 2 mm thick.

4. Characterization

Scanning electron microscopy (SEM) and OCT experiments were performed to evaluate the quality of our samples and validate the fabrication process. SEM was used to assess uniformity, wetting and good dispersion of the microspheres in the silicone matrix. In-depth cross-sections of the samples were observed. As shown in figure 3, where an image from a phantom with 7×10^9 part ml^{-1} is displayed, the microspheres are well incorporated in the silicone, are well wetted and are randomly and homogeneously distributed. The randomness in the sphere distribution is confirmed by the absence of secondary lobes to the central maximum in the 2D autocorrelation of SEM images, an example being presented in figure 4. A weak vertical linear pattern observed in the figure is caused by the unevenness induced when cutting the sample. Some SEM images indicated that a few aggregates resist the ultrasonic treatment. But in all the observed samples, these aggregates were found only at the bottom edge of the cross-sections and outside the OCT imaging region. They therefore have no effect on our results except for a very minor overestimate of the scatterer densities.

Further analysis of SEM images was also carried out to assess the control obtained over the density of scatterers. For each produced phantom, six images at the same magnification (two near the surface, two in the middle and two at the bottom of the cross section) were acquired and processed to count the number of particles in each image. This number was obtained by counting the number of finite areas with amplitude above a gray level threshold. In figure 5, we show the average number of particles per image of a phantom with respect to its nominal concentration. The results for two series of phantoms, one with particles of
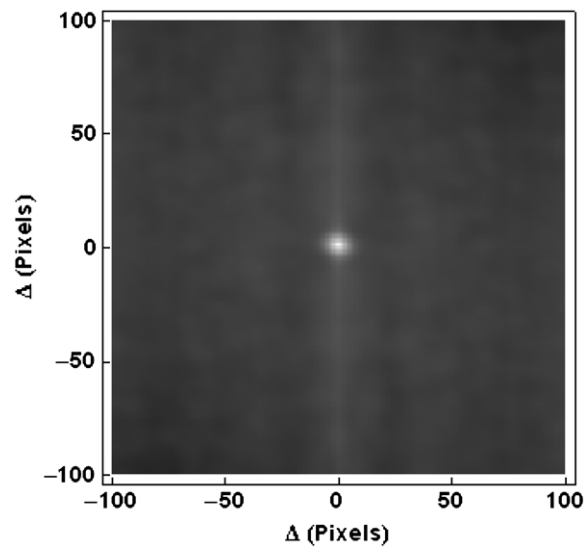
Figure 4. Two-dimensional autocorrelation of the SEM image shown in figure 3.
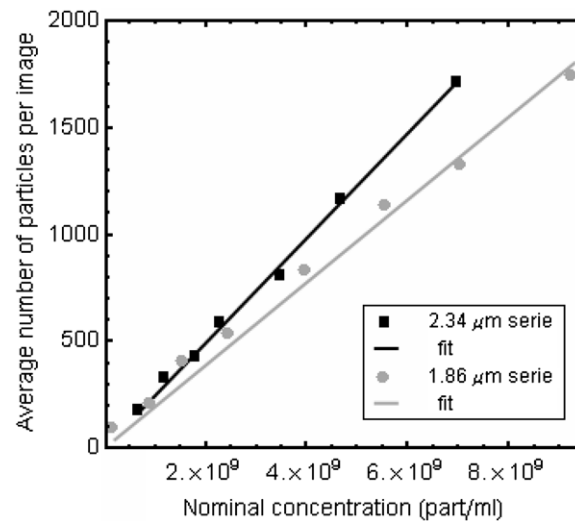

Figure 5. Relation between the number of particles evaluated from the SEM images and the nominal density of scatterers for two series of phantoms with different microsphere diameters.

1.86 μm in diameter and one with particles of 2.34 μm in diameter, are presented. Both sets show very good linearity between the number of particles in the images and the initial concentration. The difference in the slopes between the two series comes from the fact that the bigger particles have a higher chance of being uncovered when the cross section is cut. Detailed measurements (which are not shown here) also confirm that there is no variation of the concentration from top to bottom within the sample.

An additional assessment of the homogeneity and controlled distribution of the microspheres in the phantoms can be obtained from OCT measurements. A simple criterion is
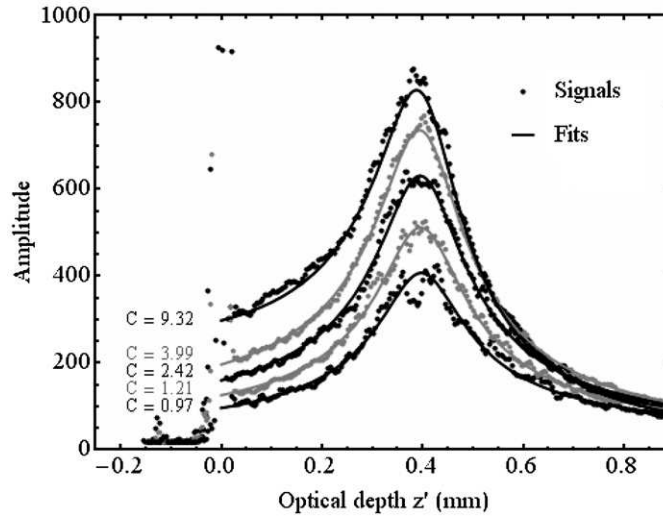
Figure 6. OCT average intensity profile for different scatterer concentrations (C, in 10^6 part mm^{-3}).

the variation of the average signal amplitude as a function of optical depth. Figure 6 presents averaged amplitude profiles measured on cross-sections 2 mm wide for five phantoms with nominal concentrations of 0.93, 1.21, 2.42, 3.99 and 9.32 × 10^6 microspheres mm^{-3}. The saturated signal near the origin comes from the air–phantom interface. The maximum observed in the vicinity of an optical depth of 0.4 mm corresponds to the focal point of the illuminating optics. The OCT signal results from the interference between the electric fields of both the reference and sample arms. Since the field in the reference arm has nearly constant amplitude during a depth scan, the variation with depth of the OCT signal amplitude depends mainly on the field in the sample arm (A_s). The amplitude A_s can be estimated by a discrete sum of phasors, each phasor corresponding to one of the many contributing scatterers. In the following, we first evaluate the contribution from each scatterer and then combine the resulting contributions.

Experiments were performed with a fiber-based OCT system. The sample was illuminated with a Gaussian beam focusing on the sample. With an illuminating Gaussian beam, the contribution a_s from each scatterer is proportional to

$$a_s \propto \frac{1}{w(z'/n)^2} \exp[-\mu(C)z'/n], \tag{1}$$

where z' is the optical thickness (distance times refractive index) relative to the sample interface, n is the refractive index of the sample, $w(z')$ is the waist of the illuminating beam and $\mu(C)$ is the attenuation coefficient that is dependent upon the microsphere concentration C. Equation (1) is obtained by first considering illumination which provides an incoming field of amplitude proportional to $\exp[-\mu(C)z'/(2n)]/w(z')$ on a microsphere, taking into account the propagation of the Gaussian beam in the sample (Siegman 1986) and the attenuation of the incoming beam due to the scattering and absorption. In the exponential, the optical thickness z' is divided by the refractive index to recover the geometric thickness. There is also a denominator 2 in the exponential to take into account that the scattering coefficient is

defined for the intensity and that a_s corresponds to a field. The variation with the depth of the waist of the Gaussian beam is given by the usual relation

$$w(z') = w_0\sqrt{1 + \left(\frac{z'/n - z_f}{z_r}\right)^2}, \tag{2}$$

where w_0 is the minimum waist, z_f is the position of the focal point in the medium and z_r is the Rayleigh distance. In equation (2), z_f and z_r are geometric lengths while z' is an optical thickness. According to a simple discrete scatterer model, a microsphere backscatters a spherical wave to be collected by the same optics used in illumination. From the optical reciprocity, the backscattered signal is also multiplied by $\exp[-\mu(C)z'/(2n)]/w(z')$ upon collection, taking into account the attenuation decay due to the propagation in the material and the backpropagation in the optical system. Combining illumination and detection leads to equation (1).

The number of contributing scatterers is proportional to the product of the microsphere concentration (C) and the volume defined by the OCT resolution length, l_c, times a transverse area of radius $w(z')$. Assuming a high density of scatterers and a fully developed speckle field, the discrete sum of phasors leads to an amplitude that is proportional to the square root of the number of contributors (Goodman 2007). Taking into account explicitly the dependences upon concentration and depth, we obtain for the total OCT signal

$$A_s(z') \propto \frac{\sqrt{C w(z'/n)^2}}{w(z'/n)^2} \exp[-\mu(C)z'/n]$$

$$\propto \frac{\sqrt{C}}{w(z'/n)} \exp[-\mu(C)z'/n]. \tag{3}$$

Based on this expression, all the experimental measurements in figure 6 were fitted with the model

$$A(z') = \frac{K}{\sqrt{1 + \left(\frac{z'/n - z_f}{z_r}\right)^2}} \exp[-\alpha z'/n] + B, \tag{4}$$

where K, z_f and α are fitting parameters. The noise level B is evaluated from the signal before the strong reflection at the air–sample interface and the value of the Rayleigh distance z_r was measured independently. All the fits obtained with the model are shown as continuous lines in figure 6. At a first glance, we see that the agreement between the experimental results and the fits is quite good over the depth of the measurement. This is another confirmation of the homogeneity in the distribution of the scatterers. Additionally, figure 7 shows the variation of the amplitude factor, K, and the attenuation parameter, α, with the concentration. As suggested by equation (3), the factor K increases as the square root of the concentration. Additionally, the attenuation parameter α varies linearly with the concentration. This is expected for a weakly scattering structure with negligible absorption (Tuchin 2000). These measured variations in K and α with concentration provide an additional confirmation of the good control over the density of scatterers.

5. Discussion

The essential requirements for phantoms to be useful in our experiments on speckle size analysis and elastography are (1) the control over the density of scatterers and (2) the deformability. The first one is achieved by the use of microspheres, which makes it possible to calculate the number of particles in the phantoms using the mass and the volume of
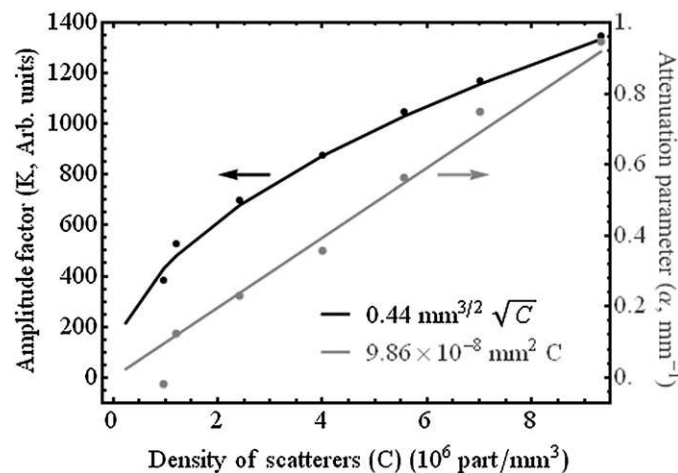
Figure 7. Variation of the amplitude factor K and attenuation coefficient α with concentration, and comparison with the model.

microspheres and silicone. The second comes from the choice of silicone as the phantom matrix. This choice of scatterer–matrix combination also leads to a very good durability of our phantoms. The phantoms fabricated a year ago are still routinely used. This is a great practical advantage.

In addition, our technique offers other possibilities. With Mie theory, it would be possible to predict the absorption, scattering and anisotropy coefficients of the phantoms based on the refractive indices and the size of the microspheres with a good agreement (Sukowski *et al* 1996, Firbank *et al* 1995). To do so, a more precise evaluation of the refractive index of the microspheres is needed. This information is not provided by the manufacturer and it has not yet been measured. Also, the complexity of the microstructure could be increased by using various sizes of microspheres. This way, a good control over the density, shape and size of the scatterers would still be achievable, and more tissue-like anisotropy and depolarization of the light could be obtained (Ghosh *et al* 2003, Gélébart *et al* 1996).

Aside from optical properties, the use of a silicone matrix allows some tissue-like mechanical properties to be reproduced as well. The most obvious is the shape of an organ. The only requirement is the availability of a proper mold. For example, figure 8 shows two of our phantoms. On the left, we show a disk-shaped phantom from which a portion was removed for SEM observation. On the right, we show a phantom with an artery shape that is used to test our catheterized OCT probes. Another interesting feature is that the elasticity of the silicone can be adjusted to some extent. We previously performed uniaxial tensile tests on silicone blank samples and on phantoms where the ratio of resin to catalyst was varied from 10:1 to 15:1. In the elastic regime, the elastic modulus was decreased from 1.1 to 0.5 MPa. We also observed strain hardening and hysteresis, two properties also common to biological tissues (Bisaillon *et al* 2008).

The step index between the scatterers and the matrix is in the range expected for biological tissues (Schmitt and Knuttel 1997). However, with low densities of scatterers, this low step index leads to a weak backscattering signal which imposes highly optimized experimental conditions. In an effort to increase the scattering signal, the silica microspheres were replaced by melamine formaldehyde microspheres, also in dry form with a much higher refractive index of $n = 1.69$. However, the experiment was not fully successful since the ultrasonic treatment
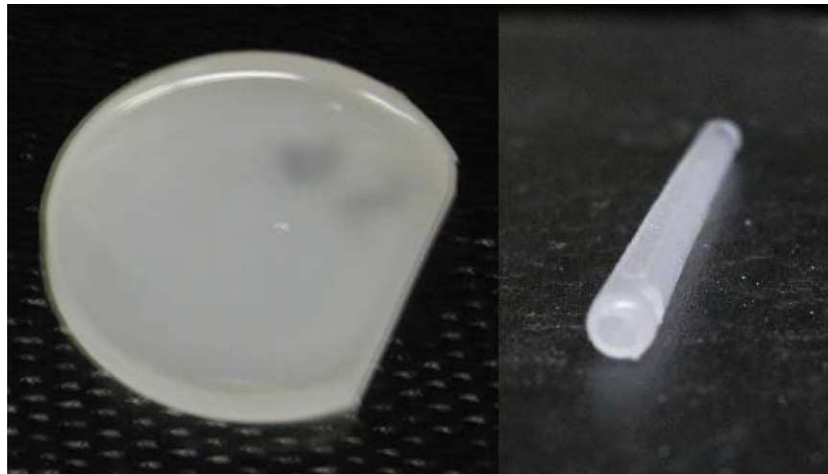
Figure 8. On the left, a disk-shaped phantom of silica microspheres in silicone and, on the right, an artery-shaped phantom of silica microspheres in silicone.

was not able to adequately break down the aggregates. In addition, it would be preferable to increase the step index somewhat less, so as to increase the backscattered signal but to still stay close to the range expected in biological tissues. A possible solution would be to chemically modify the PDMS to adjust its index of refraction as previously proposed (Kohjiya *et al* 1990). But the success of this procedure is not guaranteed with a specific product such as Sylgard 184. It might alter the transparency or the elasticity of the silicone.

6. Conclusion

To our knowledge, this is the first report of optical phantoms obtained by mixing microspheres in a silicone matrix. This combination yields phantoms with very interesting properties: simplicity of the scattering microstructure, solidity, deformability and durability. It also opens the door to more complex phantoms that could reproduce some specific optical and mechanical properties of biological tissues, while keeping a simple and well-defined microstructure. As far as our work is concerned, these phantoms led us to results showing the variation of the speckle size in OCT measurements with the density of scatterers (Bisaillon 2007, Lamouche *et al* 2008). The phantoms are routinely used to perform elastography measurements since they provide a well-defined speckle field pattern that can be tracked easily.

Copyright 2008 Government of Canada

References

Beck G C, Akgun N, Ruck A and Steiner R 1998 Design and characterisation of a tissue phantom system for optical diagnostics *Lasers Med. Sci.* **13** 160–71
Bisaillon C E 2007 Taille de speckle en tomographie par cohérence optique *Département de Génie Physique* (Montréal: École Polytechnique de Montréal)
Bisaillon C-E, Lanthier M-M, Lamouche G, Lévesque D, Maciejko R and Monchalin J-P 2008 Deformable and durable optical phantoms with controlled number of scatterers *Design and Performance Validation of Phantoms Used in Conjunction with Optical Measurements of Tissue* (San Jose, CA: SPIE)
Bouma B E and Tearney G J 2002 *Handbook of Optical Coherence Tomography* (New York: Dekker)

Dufour M L, Lamouche G, Detalle V, Gauthier B and Sammut P 2005 Low-coherence interferometry—an advanced technique for optical metrology in industry *Insight* **47** 216–9

Firbank M and Delpy D T 1993 A design for a stable and reproducible phantom for use in near infra-red imaging and spectroscopy *Phys. Med. Biol.* **38** 847–53

Firbank M, Oda M and Delpy D T 1995 An improved design for a stable and reproducible phantom material for use in near-infrared spectroscopy and imaging *Phys. Med. Biol.* **40** 955

Gélébart B, Tinet E, Tualle J-M and Avrillier S 1996 Phase function simulation in tissue phantoms: a fractal approach *Pure Appl. Opt.* A **5** 377

Ghosh N, Patel H S and Gupta P K 2003 Depolarization of light in tissue phantoms—effect of a distribution in the size of scatterers *Opt. Exp.* **11** 2198–205

Goodman J W 2007 *Speckle Phenomena in Optics—Theory and Applications* (Englewood, CO: Roberts & Company)

Gossage K W, Smith C M, Kanter E M, Hariri L P, Stone A L, Rodriguez J J, Williams S K and Barton J K 2006 Texture analysis of speckle in optical coherence tomography images of tissue phantoms *Phys. Med. Biol.* **51** 1563–75

Gossage K W, Tkaczyk T S, Rodriguez J J and Barton J K 2003 Texture analysis of optical coherence tomography images: feasibility for tissue classification *J. Biomed. Opt.* **8** 570–5

Hillman T R, Adie S G, Seemann V, Armstrong J J, Jacques S L and Sampson D D 2006 Correlation of static speckle with sample properties in optical coherence tomography *Opt. Lett.* **31** 190–2

Jiang S, Pogue B W, McBride T O and Doyley M M 2003 Near-infrared breast tomography calibration with optoelastic tissue simulating phantoms *J. Electron. Imaging.* **12** 613–20

Kohjiya S, Maeda K, Yamashita S and Shibata Y 1990 Chemical modification of silicone elastomers for optics *J. Mater. Sci.* **25** 3368–74

Lamouche G, Bisaillon C-E, Vergnole S and Monchalin J-P 2008 On the speckle size in optical coherence tomography *Coherence Domain Optical Methods and Optical Coherence Tomography in Biomedicine XII; Proc. SPIE* **6847** 684724

Lualdi M, Colombo A, Farina B, Tomatis S and Marchesini R 2001 A phantom with tissue-like optical properties in the visible and near infrared for use in photomedicine *Lasers Surg. Med.* **28** 237–43

Pogue B W and Patterson M S 2006 Review of tissue simulating phantoms for optical spectroscopy, imaging and dosimetry *J. Biomed. Opt.* **11** 041102-16

Schmitt J M and Knuttel A 1997 Model of optical coherence tomography of heterogeneous tissue *J. Opt. Soc. Am.* A **14** 1231–42

Siegman A E 1986 *Lasers* (Palo Alto, CA: University Science Books)

Sukowski U, Schubert F, Grosenick D and Rinneberg H 1996 Preparation of solid phantoms with defined scattering and absorption properties for optical tomography *Phys. Med. Biol.* **41** 1823

Tuchin V 2000 *Tissue Optics: Light Scattering Methods and Instruments for Medical Diagnosis* vol TT38 (Bellingham, WA: SPIE)

Yang H, Nguyen Q T, Ding Y, Long Y and Ping Z 2000 Investigation of poly(dimethyl siloxane) (PDMS)—solvent interactions by DSC *J. Membr. Sci.* **160** 27–43